An Ultrasensitive Photoelectrochemical Biosensor Based on $[Ru(dcbpy)_2dppz]^{2+}$/Rose Bengal Dyes Co-sensitized Fullerene for DNA Detection

Haihua Wang, Mengjie Li, Yingning Zheng, Tao Hu, Yaqin Chai, Ruo Yuan

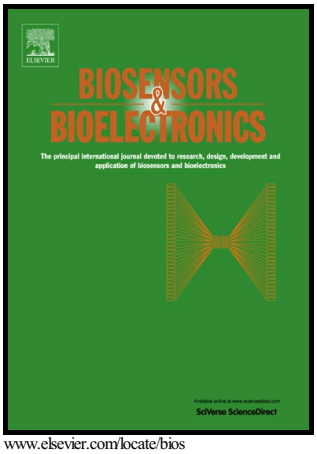

www.elsevier.com/locate/bios

PII: S0956-5663(18)30634-1
DOI: https://doi.org/10.1016/j.bios.2018.08.035
Reference: BIOS10699

To appear in: *Biosensors and Bioelectronic*

Received date: 11 June 2018
Revised date: 3 August 2018
Accepted date: 16 August 2018

Cite this article as: Haihua Wang, Mengjie Li, Yingning Zheng, Tao Hu, Yaqin Chai and Ruo Yuan, An Ultrasensitive Photoelectrochemical Biosensor Based on $[Ru(dcbpy)_2dppz]^{2+}$/Rose Bengal Dyes Co-sensitized Fullerene for DNA Detection, *Biosensors and Bioelectronic,* https://doi.org/10.1016/j.bios.2018.08.035

An Ultrasensitive Photoelectrochemical Biosensor Based on $[Ru(dcbpy)_2dppz]^{2+}$/Rose Bengal Dyes Co-sensitized Fullerene for DNA Detection

Haihua Wang, Mengjie Li, Yingning Zheng, Tao Hu, Yaqin Chai*, Ruo Yuan*

Key Laboratory of Luminescence and Real-Time Analytical Chemistry (Southwest University), Ministry of Education, College of Chemistry and Chemical Engineering, Southwest University, Chongqing 400715, People's Republic of China

E-mail address: yqchai@swu.edu.cn, (Y. Q. Chai)

yuanruo@swu.edu.cn (R. Yuan)

* Corresponding author. Tel.: +86-23-68252277; Fax.: +86-23-68253172.

Abstract

Though preferable progresses have been achieved to improve the photoelectric performance of fullerene (C_{60} NPs) by sensitized structure in photoelectrochemical (PEC) field, further application inevitably suffers from the inherent scarcities of heavy metal-involved quantum dots as sensitizers containing restricted sensitization effect, complex preparation and biological toxicity. In this work, a PEC biosensor based on $[Ru(dcbpy)_2dppz]^{2+}$/Rose Bengal dyes co-sensitized C_{60} NPs was constructed for ultrasensitive DNA (a fragment sequence of p53 gene) detection. With the merits of low toxicity and accessible operation, $[Ru(dcbpy)_2dppz]^{2+}$/Rose Bengal dyes exhibited a further sensitization efficiency towards C_{60} NPs. Through modifying wide band gap C_{60} NPs with two narrower band gap dyes ($[Ru(dcbpy)_2dppz]^{2+}$ and Rose Bengal) to form a cascade-type energy band structure, the photoelectric conversion of C_{60} NPs was significantly improved and the visible light

absorption was markedly promoted, leading to an exceptional photocurrent signal. Additionally, Nt.BstNB I enzyme-assisted target recycling amplification was employed to convert a limited quantity of target to numerous SiO_2 NPs-labeled DNA sequences (the signal quencher), resulting in a sharp decrement of photocurrent since a dramatic increment of steric hindrance on the modified electrode surface, which was performed to quantitatively estimate target. The proposed PEC biosensor for DNA detection possessed a wide linear range from 0.1 fM to 1 nM with a calculated detection limit of 37 aM. This work opened up an intriguing avenue for determination of various targets such as DNAs, microRNAs and proteins, and exhibited desirable application potential in the clinic researches, cancer therapies and other related subjects.

Keywords:

Photoelectrochemical; Dyes co-sensitized; Fullerene; $[Ru(dcbpy)_2dppz]^{2+}$; Rose Bengal

1. Introduction

As an emerging and versatile analytical technique, photoelectrochemical (PEC) assay combing the merits of optical-analysis and electron-analysis has attracted general interests due to distinctive advantages, such as accessible operation, device portability, ultrahigh sensitivity and low cost (Haddour et al., 2006; Ma et al., 2014; Wang et al., 2015b; Zang et al., 2017; Zhao et al., 2014; Zhu et al., 2017). For a PEC biosensor, an ideal photoactive material with a high and stable photocurrent intensity is greatly desirable (Fan et al., 2018; Hu et al., 2018; Qiu et al., 2018; Ruan et al., 2017; Wang et al., 2017; Zheng et al., 2016a; Zhu et al., 2016). Recently, with the rise of carbon nanomaterials, fullerene (C_{60} NPs) as an eminent photoactive material has aroused extensive

attentions in PEC fields for its intrinsic properties of strong electron-accepting capacity and noticeable electronic absorption bands throughout the total UV-vis spectrum (Hu et al., 2013; Kim et al., 2015a; Kumar et al., 2014; Lian et al., 2015; Miao et al., 2014; Wang et al., 2015a). Unfortunately, a wide band gap of C_{60} NPs (2.6 eV) restricts the photoelectric conversion and further application in PEC sensing fields (Kim et al., 2015b; Li et al., 2017). To overcome the above-mentioned challenge, sensitization strategy as a fascinating approach has drawn much attention to facilitate the photoelectric conversion of C_{60} NPs for an enhanced photocurrent response. For instance, Prashant's group explored the CdSe quantum dot (QDs)-fullerene hybrid nanocomposite for effective solar energy conversion (Bang and Kamat, 2011). Using CdTe QDs to sensitize the supramolecular donor-acceptor arrays by assembly of porphyrin and C_{60}, Zhu and his partner developed an enhanced PEC immunosensing platform for CEA evaluation (Zhu et al., 2015). Recently, fullerene/CdTe QDs sensitized structure was proposed for an ultrasensitive ''on-off-on'' PEC aptasensor (Li et al., 2016). Obviously, vibrant achievements have been realized in improving the PEC performance of C_{60} NPs with introduction of Cd-based QDs sensitizers. However, as can be seen, further application of C_{60} NPs in biological systems is inevitably restricted on account of the inherent disadvantages of heavy metals-involving elements, such as limited sensitization efficiency, high toxicity, and complicated as well as time-consuming synthesis (Cao and Zhang, 2012; Hu et al., 2014; Roming et al., 2010; Tu et al., 2016). Consequently, it is highly desirable to develop new sensitizers with higher efficiency, lower toxicity and more accessible operation for C_{60} NPs sensitization to obtain superior PEC performance.

$[Ru(dcbpy)_2dppz]^{2+}$ and Rose Bengal as two organic small molecular dyes, which own general

exceptional properties containing predominant photoelectric merits, extraordinary hydrophilicity and chemical stability, have been widely used in many fields, such as photo-oxidation technique (Li et al., 2000), photo-physical property (Sun et al., 2010), electrochemiluminescence biosensor (Wang et al., 2016). In addition, these two photoactive materials are low toxic to refrain from the inherent drawbacks of heavy metals, and their preparation are usually accessible only referring to dissolution and ultrasonication. More importantly, compared with C_{60} NPs, the energy band gaps of $[Ru(dcbpy)_2dppz]^{2+}$ (2.379 eV) (calculated *via* B3LYP/6-31G*) and Rose Bengal (1.92 eV) (Pradhan et al., 2007) are much narrower, which could match well with the energy band gap of C_{60} NPs. In this sense, a dyes co-sensitized platform could be presented by employing $[Ru(dcbpy)_2dppz]^{2+}$ and Rose Bengal to sensitize C_{60} NPs with appropriate band gap positions for a cascade-type energy band structure. This cascade-type energy band structure could adequately absorb the light energy, dramatically facilitate charge separation, and effectively inhibit the electron-hole recombination, leading to an improved photoelectric conversion efficiency and significantly enhanced photocurrent intensity of the sensing electrode. As a consequence, $[Ru(dcbpy)_2dppz]^{2+}$ and Rose Bengal could be perceived as desirable candidates to achieve favorable sensitization toward C_{60} NPs.

Herein, an ultrasensitive PEC biosensor was developed based on $[Ru(dcbpy)_2dppz]^{2+}$/Rose Bengal dyes co-sensitized C_{60} NPs structure as photoactive indicator and SiO_2 NPs-labeled DNA sequences (output) as efficient quenching element for DNA (a fragment of p53 gene) detection, which was depicted in Scheme 1. Coupling wide band gap C_{60} NPs with narrow band gaps $[Ru(dcbpy)_2dppz]^{2+}$ and Rose Bengal, a dyes co-sensitized proposal was successfully presented to

form a cascade-type energy band structure, resulting in an improved photoelectric conversion efficiency and furthermore an excellent initial photocurrent response. Additionally, the Nt.BstNB I enzyme-assisted target recycling amplification was adopted to convert a limited number of target (input) to abundant output. After output hybridized with capture on the modified electrode surface, the photocurrent response would decrease sharply due to a dramatic increment of steric hindrance, which was performed to quantitatively estimate target. This presented strategy developed a promising method for ultrasensitive detection of biomarkers, and provided a possible route to design high performance PEC biosensor.

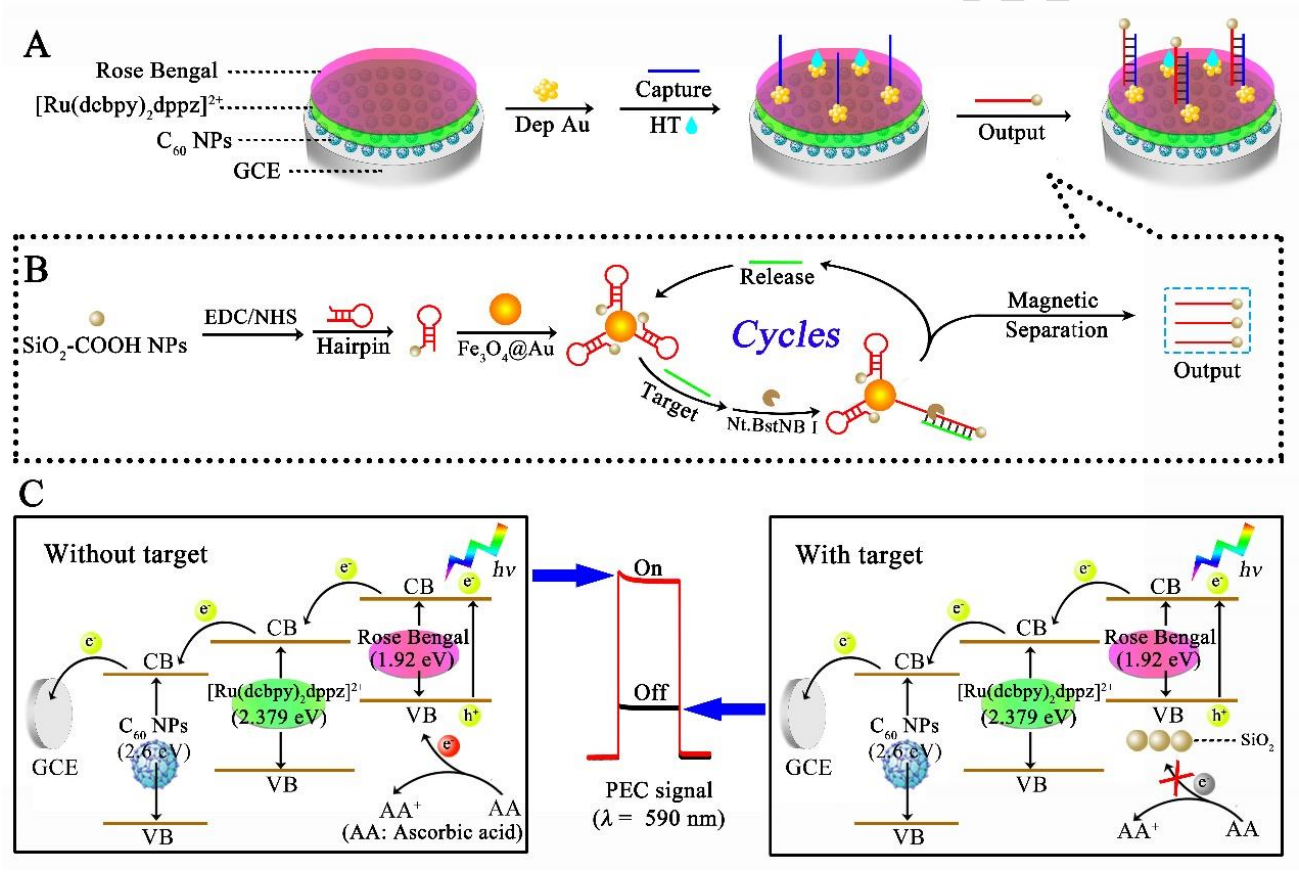

Scheme 1 Schematic illustration of (A) the fabrication process of the PEC biosensor, (B) the enzyme-assisted target recycling amplification and (C) the photocurrent response mechanism of the PEC biosensor.

2. Experimental Section

2.1. Materials and Reagents

Fullerene (C_{60} NPs) was bought from J&K Scientific Ltd. (Beijing, China). Bis(4,4′-dicarboxyl-2,2′-bibpyridyl) (4,5,9,14-tetraaza-benzo[b]-triphenylene) ruthenium(II) {$[Ru(dcbpy)_2dppz]^{2+}$} was acquired from Suna Tech Inc. (Suzhou, China). Rose Bengal (4,5,6,7-tetrachloro-2',4',5',7'-tetraiodofluorescein) was purchased from Aladdin Reagent Company (Shanghai, China). Hexanethiol (HT), gold chloride tetrahydrate ($HAuCl_4 \cdot 4H_2O$), tetraethyl orthosilane (TEOS), 3-aminopropyl triethoxysilane (APTES), N, N-Dimethylformamide (DMF), ammonium hydroxide ($NH_3 \cdot H_2O$) (28 %) and succinic anhydride were bought from Sigma Chemical Co. (St. Louis. MO, USA). Amido-modified Fe_3O_4 (Fe_3O_4-NH_2) magnetic microspheres were purchased from Tianjin BaseLine ChromTech Research Centre (Tianjin, China). N-hydroxy succinimide (NHS) and N-(3-dimethylaminopropyl)-N-ethylcarbodiimide hydrochloride (EDC) were obtained from Shanghai Medpep Co., Ltd (Shanghai, China). Ascorbic acid (AA) was gained from Sinopharm Chemical Reagent Co. Ltd. (Shanghai, China). $K_3[Fe(CN)_6]$ and $K_4[Fe(CN)_6]$ were obtained from Beijing Chemical Reagent Co. (Beijing, China). 0.1 M KCl, 0.1 M NaOH, 0.1 M KH_2PO_4 and 0.1 M Na_2HPO_4 were used to prepare 0.1 M phosphate buffered solution (PBS). The Nt.BstNB I enzyme and 10 × NE Buffer were acquired from New England Bio-labs (Ipswich, USA). The human real serum samples used for preliminary application of the PEC biosensor were obtained from the Ninth People's Hospital of Chongqing (Chongqing, China), which were isolated from the whole blood by the centrifugation at 3000 rpm for 20 min and kept frozen at -80 °C for further use.

The Hela cells were purchased from the Cell bank of type culture collection of the Chinese Academy of Science (Shanghai, China).

2.2 Preparation of C60 NPs, Fe3O4@Au NPs and Rose Bengal

C_{60} NPs and Fe_3O_4@Au NPs were prepared according to our previous reports. (Li et al., 2016; Xie et al., 2016). For Rose Bengal solution preparation, 1 mg Rose Bengal powder was placed in 10 mL deionized water with ultrasonication to get homogeneous solution. The resulted Rose Bengal solution was stored in the dark at room temperature for further use.

2.3 Preparation of Fe_3O_4@Au NPs-hairpin-SiO_2 NPs Conjugates

Firstly, 20 μL SiO_2-COOH NPs (Preparation details are exhibited in the Supplementary Material) was mixed with 8 μL EDC/NHS and the mixture was stirred for 0.5 h at room temperature to activate carboxylic-function groups. Then 5 μL hairpin (2.5 μM) labeled by amino-function groups was added and the obtained solution was stirred for 1 h to gain hairpin-SiO_2 NPs conjugates by the classic condensation reaction between carboxyl and amino. Afterwards, the resulted hairpin-SiO_2 NPs conjugates were mixed with 6 μL Fe_3O_4@Au NPs and stirred at room temperature for 16 h, leading the conjugates covalently attached to the surface of Fe_3O_4@Au NPs *via* Au-S bonds. Finally, the obtained Fe_3O_4@Au NPs-hairpin-SiO_2 NPs conjugates were stored at 4 ºC for further use.

2.4 The Nt.BstNB I Enzyme-assisted Target Recycling Amplification

Briefly, 8 μL 10 × NE Buffer and 5 μL target were added into 37 μL Fe_3O_4@Au NPs-hairpin-SiO_2 NPs solution. After hybridization at 37 ºC for 0.5 h, 4 μL Nt.BstNB I enzyme (10 units μL) was introduced and incubated at 55 ºC for 1 h, which could specifically cleave only one strand of a double stranded DNA base away from the 3′-end of its recognition sequence (5′ -GAGTC-3′). Then, the mixture was heated to 80 ºC and kept for 20 mins to deactivate the Nt.BstNB I enzyme. After cooling down to room temperature naturally, the supernatant was collected by magnetic separation.

2.5 Fabrication of the PEC Biosensor

Prior to use, the bare GCE was polished with 0.3 μm and 0.05 μm alumina paste, respectively, and ultrasonically cleaned in deionized water and ethanol to get a mirror-like surface (Liang et al., 2015). Subsequently, 6 μL C_{60} NPs, 6 μL $[Ru(dcbpy)_2dppz]^{2+}$ and 6 μL Rose Bengal solution were dropped onto the pretreated electrode step by step. After incubated at 37 ℃ to get thin films, the modified electrode was electrodeposited in 1 % $HAuCl_4$ solution at -0.2 V for 4 s to obtain an Au NPs layer (Dep Au). Next, 20 μL 2.5 μM capture was attached to the electrode surface at room temperature for 16 h through Au-S bonds. Then, the modified electrode was incubated with 10 μL 1 mM HT for 1 h to block nonspecific binding sites. Finally, the modified electrode was incubated with 20 μL output to hybridize with capture at 37 ºC for 2 h. After each step, the electrode was thoroughly cleaned with deionized water to remove physically absorbed species.

2.6 PEC Measurements

The PEC measurements were performed in 4 mL PBS (pH 7.4, 0.1 M) containing 0.12 M freshly prepared AA solution at room temperature. The excitation light source (wavelength: λ = 590 nm; radiant flux: Φ = 976 mW) was provided by a light-emitting diode lamp and the light was switched "off-on-off" for 10 s-20 s-10 s under 0.0 V potential.

3. Results and Discussion

3.1 Morphology Characterizations of the Nanomaterials

The morphologies of the synthesized nanomaterials were characterized by TEM. As illustrated in Figure 1A, C_{60} NPs showed globular structure with the size of 30 nm approximately. The prepared SiO_2-COOH NPs also showed globular structure and the size was about 40 nm, which was shown in Figure 1B. The characterization results indicated that C_{60} NPs and SiO_2-COOH NPs were synthesized successfully.

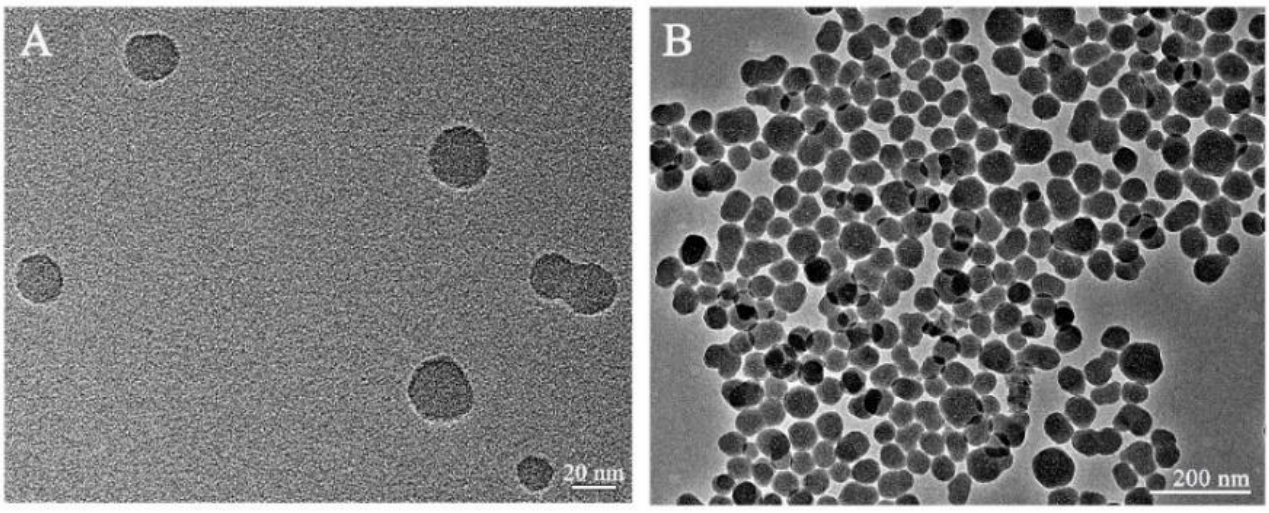

Fig. 1 TEM images of (A) C_{60} NPs and (B) SiO_2-COOH NPs.

3.2 The Co-sensitized Mechanism of the Photoactive Materials

An ultrasensitive PEC biosensor based on $[Ru(dcbpy)_2dppz]^{2+}$/Rose Bengal dyes co-sensitized C_{60} NPs for DNA detection was proposed in this work. C_{60} NPs is a promising photoactive material because of its various merits, such as strong electron-accepting capacity and the improved ability of light absorption. Nevertheless, the existence of wide band gap (2.6 eV) restricts the photoelectric transformation efficiency. In this regard, the co-sensitization strategy is an ideal and fascinating choice to improve the photoelectric conversion efficiency of C_{60} NPs (Li et al., 2017). Compared with C_{60} NPs, $[Ru(dcbpy)_2dppz]^{2+}$ (2.379 eV) and Rose Bengal (1.92 eV) possess narrower band gaps, which would match well with C_{60} NPs to form cascade-type energy band structure. The cascade-type energy band structure could adequately absorb the light energy, dramatically facilitate charge separation, and effectively inhibit the electron-hole recombination, leading to obvious increments of photoelectric conversion efficiency as well as photocurrent intensity. For the C_{60} NPs/$[Ru(dcbpy)_2dppz]^{2+}$/Rose Bengal dyes co-sensitized platform, the mechanism of photocurrent generation was depicted in Scheme 1. Briefly, under 590 nm excitation light source, electrons of Rose Bengal were firstly migrated from valence band (VB) to conduction band (CB), forming electron-hole pairs. Then the photoexcited electrons were transferred to the CBs of $[Ru(dcbpy)_2dppz]^{2+}$ and C_{60} NPs successively, and lastly delivered to the surface of bare GCE to generate a high photocurrent response. Meanwhile, AA as electrons donor could facilitate the charge separation and suppress the electron-hole pair recombination of photoactive materials, achieving an enhanced and stable photocurrent response.

3.3 CV and PEC Characterization of the PEC Biosensor

CV was employed to characterize the fabrication process of the PEC biosensor. As shown in Figure 2A, the pretreated bare GCE exhibited a couple of pretty redox peak current (curve a). When C_{60} NPs was coated on the electrode, the redox peak current decreased (curve b) because C_{60} NPs could hinder electronic transmission. After modified with $[Ru(dcbpy)_2dppz]^{2+}$, a moderate increase of the peak current was obtained (curve c), which was ascribed to the fact that abundant positive charges of $[Ru(dcbpy)_2dppz]^{2+}$ could significantly improve the ability of the negatively charged redox probe $[Fe(CN)_6]^{3-/4-}$ to access the electrode surface. Then Rose Bengal was anchored, a decrement of the peak current was acquired (curve d) since the organic small molecule Rose Bengal could block electron transfer. With the procedure of Dep Au, the peak current increased (curve e) owing to the excellent conductivity of Au NPs. When capture and HT were immobilized on the modified electrode consecutively, the peak current (curve f and curve g, respectively) showed continuous decrease because of the increased steric effect. Finally, when the modified electrode was incubated with output, the redox peak current (curve h) decreased sharply due to the significant increment of the steric hindrance on the electrode surface, which could depress the electron transfer effectively. These results indicated that the PEC biosensor was constructed successfully.

The fabrication process of the PEC biosensor was also characterized by photocurrent responses. As illustrated in Figure 2B, the photocurrent response of the bare GCE closed to zero (curve a). When C_{60} NPs was coated on the electrode, a low photocurrent response was observed (curve b) owing to a limited photoelectric conversion efficiency of C_{60} NPs. After immobilization of $[Ru(dcbpy)_2dppz]^{2+}$, an increment of the photocurrent response (curve c) was obtained due to the sensitized effect of $[Ru(dcbpy)_2dppz]^{2+}$ toward C_{60} NPs. When Rose Bengal was further modified,

the photocurrent response (curve d) took on a dramatical enhancement, which was ascribed to the synergistic effect of $[Ru(dcbpy)_2dppz]^{2+}$/Rose Bengal dyes co-sensitized C_{60} NPs. Further increment of the photocurrent response was found after Dep Au (curve e) due to the excellent conductivity of Au NPs. However, when the capture and HT were immobilized on the modified electrode, the photocurrent responses (curve f and curve g, respectively) involved consecutive decrements because of the increased steric hindrance effect. Finally, the incubation with output caused obvious inhibition of the photocurrent response (curve h), which was attributed to the significantly increment of steric hindrance from SiO_2 NPs. The results demonstrated that the PEC biosensor was fabricated conceivably.

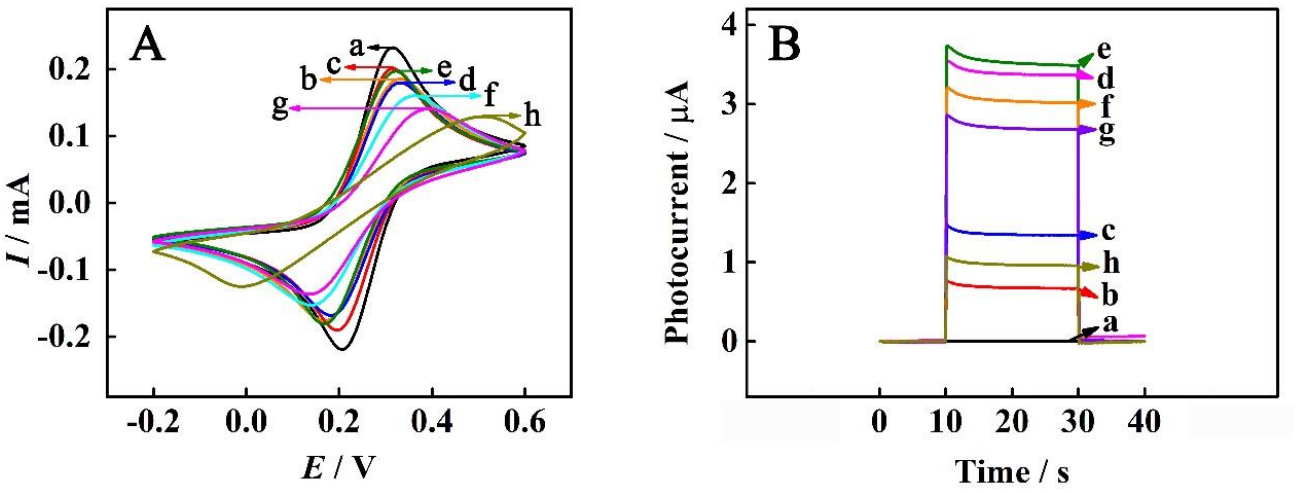

Fig. 2 CV and PEC responses of (a) bare GCE, (b) C_{60} NPs/GCE, (c) $[Ru(dcbpy)_2dppz]^{2+}$/C_{60} NPs/GCE, (d) Rose Bengal/$[Ru(dcbpy)_2dppz]^{2+}$/C_{60} NPs/GCE, (e) Dep Au/Rose Bengal/$[Ru(dcbpy)_2dppz]^{2+}$/C_{60} NPs/GCE, (f) capture/Dep Au/Rose Bengal/$[Ru(dcbpy)_2dppz]^{2+}$/C_{60} NPs/GCE, (g) HT/capture/Dep Au/Rose Bengal/$[Ru(dcbpy)_2dppz]^{2+}$/C_{60} NPs/GCE and (h) output/HT/capture/Dep Au/Rose Bengal/$[Ru(dcbpy)_2dppz]^{2+}$/C_{60} NPs/GCE. CV procedures were developed in 2 mL PBS (pH 7.0, 0.1 M) containing 5.0 mM $[Fe(CN)_6]^{3-/4-}$ and 0.1 M KCl between -0.2 and 0.6 V at a scan rate of 50 mV/s. PEC

measurements were performed in 4 mL PBS (pH 7.4, 0.1 M) containing 0.12 M AA.

3.4 PEC Detection of Target DNA

To estimate the analytical performance, the established PEC biosensor was applied to detect the target DNA (a fragment sequence of p53 gene) with different concentrations. As depicted in Figure 3, the photocurrent response decreased gradually as the concentration of the target increased. The liner range exhibited from 0.1 fM to 1 nM with a theoretical detection limit of 33 aM (defined as LOD = 3 S_B/m, where S_B and m are the standard deviation of the blank and the slope of the calibration plot at lower concentration ranges, respectively). Besides, the practical detection limit was calculated down to 37 aM (at the signal-to-noise of 3; calculation details are available in the Supplementary Material). In addition, the linear equation was I = - 0.2189 lg c + 1.091 with a correlation coefficient (R) of 0.9934 (where I was the photocurrent intensity and c was the concentration of target). Besides, the analytical performance of the fabricated PEC biosensor was compared with other reported works for DNA estimation. As depicted in Table S1 in the Supplementary Material, the proposed PEC biosensor exhibited a much lower detection limit and wider liner range, which was mainly owing to the perfect co-sensitized platform and signal amplification strategy.

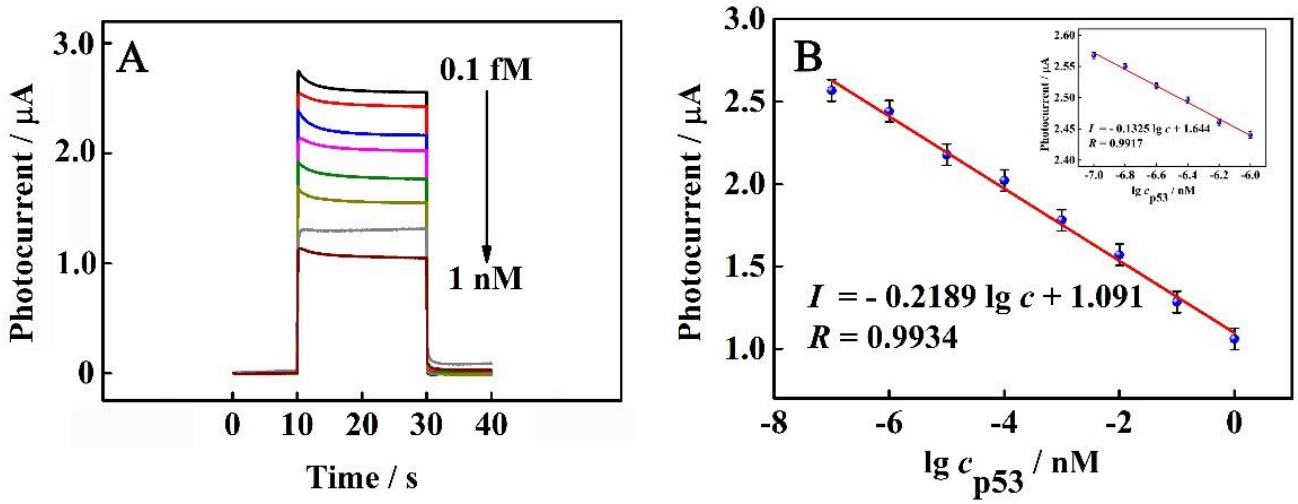

Fig. 3 (A) Photocurrent responses of the PEC biosensor incubated with target DNA of different concentrations (from top to bottom): 1.000×10^{-1} fM, 1.000 fM, 1.000×10 fM, 1.000×10^{2} fM, 1.000 pM, 1.000×10 pM, 1.000×10^{2} pM, 1.000 nM and (B) the linear relationship between photocurrent response and the logarithm of the concentration of target DNA. The insert showed the linear relationship between photocurrent response and the logarithm of the ultralow concentration of target DNA (from left to right): 1.000×10^{-7} nM, $1.000 \times 10^{-6.8}$ nM, $1.000 \times 10^{-6.6}$ nM, $1.000 \times 10^{-6.4}$ nM, $1.000 \times 10^{-6.2}$ nM and 1.000×10^{-6} nM.

3.5 Selectivity and Stability of the PEC Biosensor

The selectivity of the PEC biosensor was performed by using single-base mismatch DNA 1 (smDNA 1) (100 nM), single-base mismatch DNA 1 (smDNA 2) (100 nM) and double-bases mismatch DNA (dmDNA) (100 nM) as interfering substances. As depicted in Figure 4A, compared with the photocurrent response for these interferences, a sharp decrease of the photocurrent response for target (1 nM) was obtained. The result indicated that the PEC biosensor possessed perfect selectivity. The stability of the PEC biosensor was conducted with 1 pM target under periodic off-on-off light for 10 cycles. As shown in Figure 4B, the relative standard deviation (RSD)

for photocurrent response was 2.46 %, which suggested that the proposed PEC biosensor possessed excellent stability.

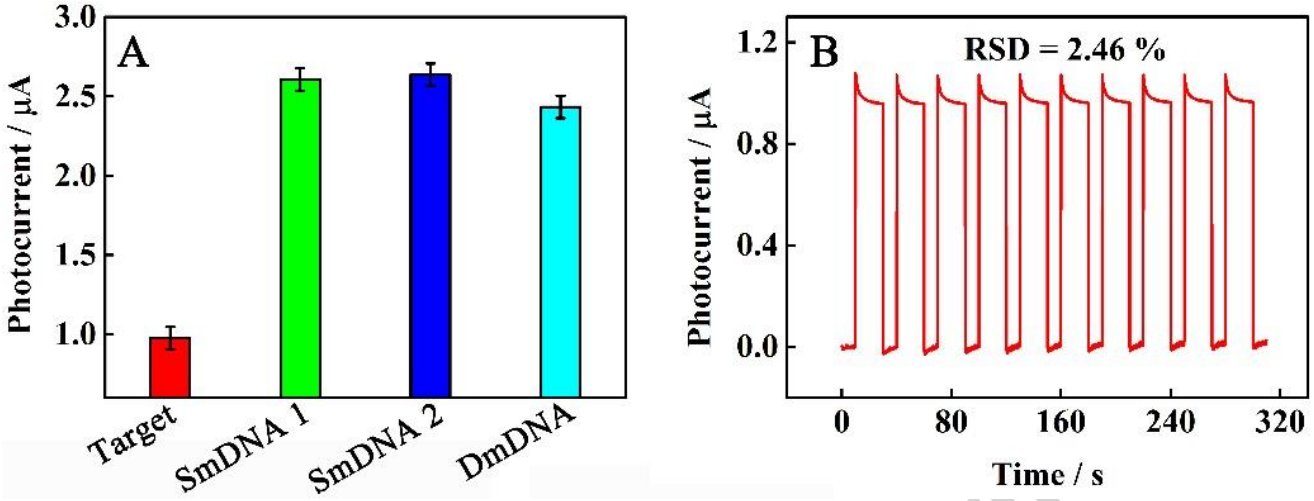

Fig. 4 (A) Selectivity of the PEC biosensor incubated with different sequences: target, smDNA 1, smDNA 2, dmDNA and (B) stability of the PEC biosensor incubated with 1 pM target.

3.6 The Application of the PEC Biosensor for DNA Evaluation in Human Blood Serum Samples and Hela cell Samples

The preliminary feasibility of the proposed PEC biosensor was validated by usage of the human blood serum samples (provided by the Ninth People's Hospital of Chongqing, China). Prior to use, the serum samples were diluted 10 times with PBS buffer (pH = 7.0) to get a diluted samples (10 %), followed by adding target sequences with a range of different concentrations. As tabulated in Table S2 in the Supplementary Material, the recovery ranged from 92.00 to 108.00 %, which suggested the proposed PEC biosensor possessed effective and reliable performance for DNA determination in biomedical analysis and clinic researches.

The applicability and capability of the proposed PEC biosensor was further verified in Hela

cell samples based on our previous report (Zheng et al., 2016b) with major modifications. In the light of the literatures (Prusty and Das, 2005; Balasubramanyam et al., 2004; Fang et al., 2005), curcumin as the anti-tumor indicator for some cancer cells has a positive effect on the existence of p53 gene fragment in per Hela cell, which can be performed to evaluate the applicability of the PEC biosensor. As depicted in Figure S4 in the Supplementary Material, the concentration of p53 gene fragment revealed obvious increments as the curcumin induced in Hela cell increased. The variation trend of the results were consistent with the previous research, which suggested that the fabricated PEC biosensor possessed a great potential for ultrasensitive estimation of genes in cell samples for early diagnosis of cancers.

4. Conclusions

In summary, an ultrasensitive PEC biosensor for DNA detection was presented based on the cascade-type energy band structure consisting of the photoactive material C_{60} NPs with its sensitizers $[Ru(dcbpy)_2dppz]^{2+}$/Rose Bengal, and enzyme-assisted target recycling amplification strategy for improved detection sensitivity and extended linear range. As the co-sensitized platform leading to approximately 5-fold enhancement of photocurrent intensity versus C_{60} NPs alone, the well-established PEC biosensor exhibited a wide liner range from 0.1 fM to 1 nM with an ultralow detection limit of 37 aM. In addition, the proposed PEC biosensor indicated desirable potentiality for DNA determination in human blood serums and Hela cells, which submitted universal approach to determine other models and related subjects. Whereas the detection limit and sensitivity in this work were still unsatisfying compared to several literatures using PEC technique for p53 gene

research (Yang et al., 2016) and DNA detection (Shi et al., 2018), super-performance photoactive materials and cascade amplification of target DNA will draw much attention in our future research.

Acknowledgements

This work was financially supported by the NNSF of China (21575116, 21675129, 51473136, 21775124) and the Fundamental Research Funds for the Central Universities (XDJK2018AA003), China.

References

Balasubramanyam, K., Varier, R.A., Altaf, M., Swaminathan, V., Siddappa, N.B., Ranga, U., Kundu, T.K., 2004. J. Biol. Chem. 49, 51163-51178.

Bang, J.H., Kamat, P.V., 2011. ACS Nano 5, 9421-9427.

Cao, P., Zhang, C.Y., 2012. Anal. Chem. 84, 6199-6205.

Fan, D.W., Bao, C.Z., Khan, M.S., Wang, C.L., Zhang, Y., Liu, Q.Z., Zhang, X., Wei, Q., 2018. Biosens. Bioelectron. 106, 14-20.

Fang, J.G., Lu, J., Holmgren, A., 2005. J. Biol. Chem. 280, 25284-25290

Haddour, N., Chauvin, J., Gondran, C., Cosnier, S., 2006. J. Am. Chem. Soc. 128, 9693-9698.

Hu, C.G., Zheng, J.N., Su, X.Y., Wang, J., Wu, W.Z., Hu, S.S., 2013. Anal. Chem. 85, 10612-10619.

Hu, R., Zhang, X.B., Zhao, Z.L., Zhu, G.Z., Chen, T., Fu, T., Tan, W.H., 2014. Angew. Chem. 126, 5931-5936.

Hu, T., Zheng, Y.N., Li, M.J., Liang, W.B., Chai, Y.Q., Yuan, R., 2018. Anal. Chem. 90, 6096-6101.

Kim, J.K., Bae, S., Kim, W.J., Jeong, M.J., Lee, S.H., Lee, C.L., Choi, W.K., Hwang, J.Y., Park, J.H., Son, D.I., 2015a. Nano Energy 13, 258-266.

Kim, K., Lee, T.H., Santos, E.J.G., Jo, P.S., Salleo, A., Nishi, Y., Bao, Z.N., 2015b. ACS Nano 9, 5922-5928.

Kumar, P., Narayanan, R., Deepa, M., Srivastava, A.K., 2014. J. Mater. Chem. A 2, 9771-9783.

Li, M.J., Zheng, Y.N., Liang, W.B., Yuan, R., Chai, Y.Q., 2017. ACS Appl. Mater. Interfaces 9, 42111-42120.

Li, M.J., Zheng, Y.N., Liang, W.B., Yuan, Y.L., Chai, Y.Q., Yuan, R., 2016. Chem. Commun. 52, 8138-8141.

Li, X.Z., Liu, H.L., Yue, P.T., Sun, Y.P., 2000. Environ. Sci. Technol. 34, 4401-4406.

Lian, Z., Xu, P., Wang, W., Zhang, D., Xiao, S., Li, X., Li, G., 2015, ACS Appl. Mater. Interfaces 7, 4533-4540.

Liang, W.B., Zhuo, Y., Xiong, C.Y., Zheng, Y.N., Chai, Y.Q., Yuan, R., 2015. Anal. Chem. 87, 12363-12371.

Ma, Z.Y., Pan, J.B., Lu, C.Y., Zhao, W.W., Xu, J.J., Chen, H.Y., 2014. Chem. Commun. 50, 12088-12090.

Miao, Y., Xu, J., Shen, Y., Chen, L., Bian, Y., Hu, Y., Zhou, W., Zheng, F., Man, N., Shen, Y., Zhang, Y., Wang, M., Wen, L., 2014. ACS Nano 8, 6131-6144.

Pradhan, B., Batabyal, SK., Pal, AJ., 2007. Sol. Energy Mater. Sol. Cells 91, 769-773.

Prusty, B.K., Das, B.C., 2005. Int. J. Cancer 113, 951-960.

Qiu, Z. L., Shu, J., Tang, D.P., 2018. Anal. Chem. 90, 1021-1028.

Roming, M., Lünsdorf, H., K. E. J. Dittmar and Feldmann, 2010. Angew. Chem., Int. Ed. 49, 632-637.

Ruan, Y.F., Zhang, N., Zhu, Y.C., Zhao, W.W., Xu, J.J., Chen, H.Y., 2017. Anal. Chem. 89, 7869-7875.

Shi, X.M., Fan, G.C., Tang, X., Shen, Q., Zhu, J.J., 2018. Biosens. Bioelectron. 109, 190-196.

Sun, Y., Collins, J.S. N., Joyce, L.E., Turro, C., 2010. Inorg. Chem. 49, 4257-4262.

Tu, W.W., Cao, H.J., Zhang, L., Bao, J.C., Liu, X.H., Dai, Z.H., 2016. Anal. Chem. 88, 10459-10465.

Wang, H.J., Yuan, Y.L., Zhuo, Y., Chai, Y.Q., Yuan, R., 2016. Anal. Chem. 88, 5797-5803.

Wang, J., Liu, Z., Hu, C., Hu, S., 2015a, Anal. Chem. 87, 9368-9375.

Wang, L.N., Han, D.X., Ni, S., Ma, W.G., Wang, W., Niu, L., 2015b. Chem. Sci. 6, 6632-6638.

Wang, Y.H., Ge, S.G., Zhang, L.N., Yu, J.H., Yan, M., Huang, J.D., 2017. Biosens. Bioelectron. 89, 859-865.

Xie, S.B., Dong, Y.W., Yuan, Y.L., Chai, Y.Q., Yuan, R., 2016. Anal. Chem. 88, 5218-5224.

Yang, L., Tao, Y., Yue, G., Li, R., Qiu, B., Guo, L., Lin, Z., Yang, H.H., 2016. Anal. Chem. 88, 5097-5103.

Zang, Y., Lei, J.P., Ju, H.X., 2017. Biosens. Bioelectron. 96, 8-16.

Zhao, W.W., Xu J.J., Chen, H.Y., 2014. Chem. Rev. 114, 7421-7441.

Zheng, Y.N., Liang, W.B., Xiong, C.Y., Yuan, Y.L., Chai, Y.Q., Yuan. R., 2016a. Anal. Chem. 81, 423-430.

Zheng, Y.N., Liang, W.B., Yuan, Y.L., Xiong, C.Y., Xie, S.B., Wang, H.J., Chai, Y.Q., Yuan. R.,

2016b. Biosens. Bioelectron. 81, 423-430.

Zhu, C.Z., Du, D., Lin, Y.H., 2017. Biosens. Bioelectron. 89, 43-55.

Zhu, H., Fan, G.C., Abdel-Halim, E.S., Zhang, J.R., Zhu, J.J., 2016. Biosens. Bioelectron. 77, 339-346.

Zhu, P., Wang, P., Kan, L., Sun, G., Zhang, Y., Yu, J., 2015. Biosens. Bioelectron. 68, 604-610.

High Lights:

- The $[Ru(dcbpy)_2dppz]^{2+}$/Rose Bengal dyes co-sensitized fullerene platform exhibited significant PEC performance for an improved detection sensitivity and extended linear range.
- $[Ru(dcbpy)_2dppz]^{2+}$ and Rose Bengal were low toxic, and their preparation were usually accessible.
- The Nt.BstNB I enzyme-assisted target recycling amplification and the quencher elements SiO_2 NPs were introduced for quantitative detection of target DNA.